Comment on "Abyssal Upwelling and Downwelling Driven by Near-Boundary Mixing"

JAMES R. LEDWELL

Woods Hole Oceanographic Institution, Woods Hole, Massachusetts

(Manuscript received 2 May 2017, in final form 18 December 2017)

ABSTRACT

McDougall and Ferrari have estimated the global deep upward diapycnal flow in the boundary layer overlying continental slopes that must balance both downward diapycnal flow in the deep interior and the formation of bottom water around Antarctica. The decrease of perimeter of isopycnal surfaces with depth and the observed decay with height above bottom of turbulent dissipation in the deep ocean play a key role in their estimate. They argue that because the perimeter of seamounts increases with depth, the net effect of mixing around seamounts is to produce net downward diapycnal flow. While this is true along much of a seamount, it is shown here that diapycnal flow of the densest water around the seamount is upward, with buoyancy being transferred from water just above. The same is true for midocean ridges, whose perimeter is constant with depth. It is argued that mixing around seamounts and especially midocean ridges contributes positively to the global deep overturning circulation, reducing the amount of turbulence demanded over the continental slopes to balance the buoyancy budget for the bottom and deep water.

Attention has been drawn recently to the implications of a positive divergence of buoyancy flux prevailing in much of the interior of the deep ocean estimated from vertical profiles of turbulent kinetic energy dissipation (DeLavergne et al. 2016; Ferrari et al. 2016). The diapycnal flow in the interior is therefore to greater neutral density (i.e., downward), in the opposite direction to that needed to balance the production of bottom water around Antarctica. Convergence of buoyancy due to turbulent buoyancy flux and geothermal heating in a boundary layer along the abyssal plains and along continental slopes and other topographic features must therefore be strong enough to balance the interior downward diapycnal flow, in addition to balancing the production of bottom water.

McDougall and Ferrari (2017, hereinafter MF17), following up on this work, estimate how large this upward diapycnal flow in the bottom boundary layer must be, and they estimate the order of magnitude of the average diapycnal diffusivity needed at the top of the boundary layer over the continental slopes. They also show clearly how the hypsometry of ocean basins facilitates overturning of the deep water by offering increasing perimeter with height. Since seamounts offer decreasing perimeter with height, MF17 argue from an idealized geometry that the effect of mixing around seamounts is to increase the density of the water around them. Here I argue that while this is true along much of a seamount, near the base of a seamount the fluid is made lighter. In steady state, the total rate of change of buoyancy in a cylindrical control volume enclosing a seamount is slightly positive, equal to the diffusive flux through a neutral density surface delimiting the top of the control volume, plus the geothermal flux at the bottom. Thus, loss of buoyancy by fluid along the seamount at middepths is balanced by gain of buoyancy by the fluid in the bottom layer at the base of the seamount.

There are many seamounts in the global ocean. Abyssal waters may move from one seamount to another, becoming more buoyant as they travel farther from their source. Hence, seamounts may play a positive role in lightening bottom water in the deep cell of the meridional overturning circulation. More importantly, the same is true of diapycnal mixing on the flanks of midocean ridges, whose gross perimeter is roughly constant with depth. Mixing along the flanks of midocean ridges may in fact carry a large part of the burden

Corresponding author: James R. Ledwell, jledwell@whoi.edu

DOI: 10.1175/JPO-D-17-0089.1

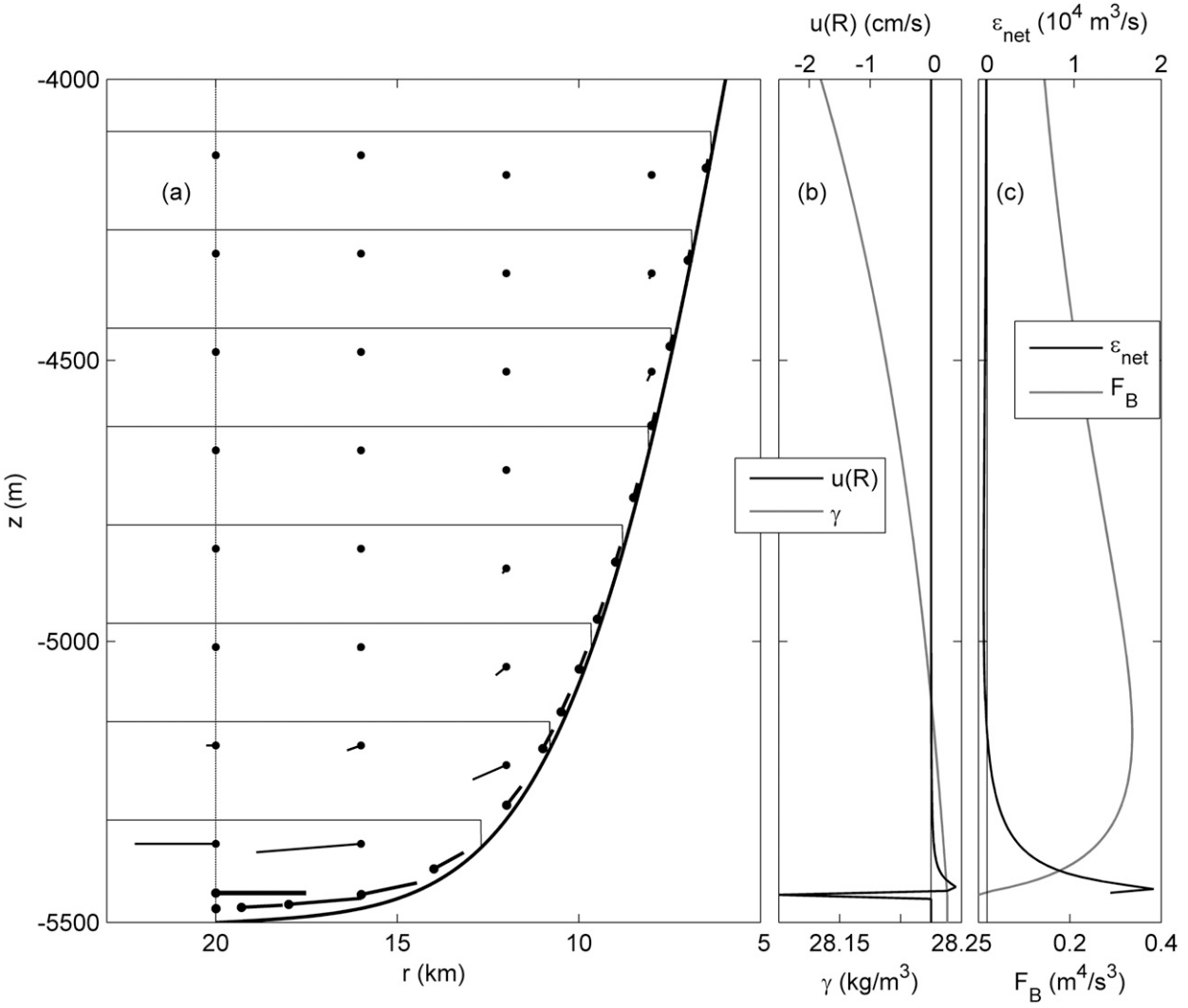

FIG. 1. Idealized circulation along the deep flank of a radially symmetric seamount. (a) The heavy black curve shows the bottom. The light lines show isopycnal surfaces, which are horizontal outside of the top of the boundary layer and then dip down in the 49-m-deep boundary layer at right angles to the bottom (angles are distorted by vertical exaggeration). The vertical line at $r = 20$ km shows the left edge of the model domain. Line segments represent velocity vectors, with a dot at their tails. The inward horizontal velocity of -2.5 cm s^{-1} 52 m off the bottom at $r = 20$ km is confined to the 7-m-thick model layer just above the boundary layer. The length of this vector has been attenuated by a factor of 50 compared with the lengths of the vectors representing the flow in the interior. The vectors in the boundary layer have been attenuated by 10 and are all toward the seamount (maximum = 0.4 cm s^{-1} near 18 km). Diapycnal diffusivity, and therefore the boundary layer velocity, is 0 at $r = 20$ km and beyond, by construction. Velocities between 4000 m and the seamount top at 2461 m are small. (b) Radial velocity u at the outer boundary of the domain is shown as a black line (top axis; the fine vertical line is at $u = 0$ for reference). The neutral density used in the calculation is shown as a gray curve (bottom axis). Fluid is exported between $z = -4877$ and -5444 m and weakly imported above -4877 m. (c) The gray line shows the area-integrated diffusive buoyancy flux F_B (bottom scale), and the black line shows the net upward diapycnal volume flux $\varepsilon_{\mathrm{NET}}$ (top scale), with a fine line at $\varepsilon_{\mathrm{NET}} = 0$ shown for reference.

of lightening the bottom water, reducing the burden inferred by MF17 for mixing along continental slopes.

To clarify the situation around a seamount, consider a cylindrically symmetric seamount around which the density field and mean flow field are also cylindrically symmetric and steady. Consider the cross-slope fluxes of mass and buoyancy in the domain shown in Fig. 1a. Ignore the details of the isopycnal lines for the moment. At the top of the domain is a neutral density surface through which there is a diffusive buoyancy flux and an advective mass flux due to convergence of this diffusive flux. These fluxes are weak, so let us ignore them for simplicity, as done by MF17. At the sides, at radius R, isopycnal surfaces enter the volume; I will not yet specify their shape inside the volume, or the flow along them and across them, except to note that if the stratification is

stable the geometry of the situation requires the deeper of these isopycnal surfaces to intersect the sloping bottom on the flanks of the seamount so that density decreases along the bottom toward the seamount. Let there be a layer of height h_b just above the bottom within which isopycnal surfaces are perpendicular to the bottom and at the top of which there is a nonnegative downward turbulent flux of buoyancy. Make the reasonable assumption that convergence of buoyancy flux by along-bottom eddy mixing is negligible compared with this quasi-vertical flux, as in MF17. In that case, fluid in this boundary layer must flow toward regions of lighter density to balance the sum of the downward buoyancy flux from above and the geothermal buoyancy flux from below. So, in this steady-state, cylindrically symmetric situation, the radial flow in the boundary layer must be upslope. Let F_V be the boundary layer volume flux in the radial direction along the perimeter at the outer edge of the control volume at $r = R$. To conserve mass we must have

$$\int_{z_b+h_b}^{z_t} u(R,z)\,dz = -F_V, \tag{1}$$

where the integral is from the top of the boundary layer at $z_b + h_b$ to the top of the control volume at z_t, and $u(R, z)$ is the radial velocity, defined to be positive outward, at the outer wall of the control volume at radius R.

Neglecting changes in density in the interior of the control volume associated with mixing in the face of the nonlinearity of the equation of state, and again neglecting also the geothermal flux and the weak fluxes at the top of the control volume, we have the following equation for the buoyancy budget for the control volume:

$$\int_{z_b+h_b}^{z_t} u(R,z)b(R,z)\,dz = -F_V\overline{b}_B, \tag{2}$$

where $b(R, z)$ is the buoyancy at the wall and $\overline{b}_B$ is the velocity-weighted mean buoyancy in the boundary layer at $r = R$.

Combining (1) and (2) we have

$$\int_{z_b+h_b}^{z_t} u(R,z)\left[b(R,z) - \overline{b}_B\right] dz = 0. \tag{3}$$

Since the buoyancy in the boundary layer is less than the buoyancy above it, the quantity in brackets is positive. Thus, there must be places along the wall, above the top of the boundary layer, at which u is negative (i.e., toward the seamount) and other places where u is positive (away from the seamount). The net effect of mixing in the region around the seamount is to lighten water entering at the greatest densities and to export and import fluid of various densities at higher levels, such that mass and buoyancy are conserved.

This analysis does not contradict the general formulas of MF17. There, the net flow through a neutral surface around a seamount is given by their (A10) and (12) [see also (26) in Klocker and McDougall (2010)]:

$$\varepsilon_{\mathrm{NET}} = dF_B/db, \tag{4}$$

where F_B is the downward diffusive buoyancy flux integrated over the neutral density surface. This flux is dominated by downward buoyancy flux in what MF17 call the stratified mixing layer above the boundary layer, with the flux decreasing with height above the top of the boundary layer.

In MF17, the buoyancy flux is integrated over an area that is large enough that the buoyancy flux becomes very small at large distance along isopycnal surfaces from the sloping bottom, because in the configurations they consider the height above the bottom becomes large, and so buoyancy flux becomes small. They have analyzed the situation for a conical seamount whose slope is constant from the peak of the seamount down to indefinite depth. Also constant in the analysis are the vertical buoyancy gradient, the buoyancy flux at the top of the bottom boundary layer, and the scale height for the decay of the buoyancy flux with height above bottom. These simplifications bring out the effect of the decreasing perimeter of the seamount with height. Since F_B is dominated by the buoyancy flux in an annulus with decreasing area with height, dF_B/db is negative and $\varepsilon_{\mathrm{NET}}$ is downward across isopycnal surfaces and is inversely proportional to the square of the bottom slope, which I will call α [see (32) in MF17]. The diapycnal volume flux $\varepsilon_{\mathrm{NET}}$ is constant on the flanks of this conical seamount. At the top, where the slope and radius both go to zero, there must be an epipycnal influx of fluid from the surroundings to feed the downward volume flux, as pointed out by McDougall (1989). There is no bottom, so the constant downward diapycnal flow goes on forever.

A more realistic case for a seamount whose slope becomes small near the peak and near the base is discussed qualitatively by MF17 (see their Fig. 6; see also McDougall 1989), by invoking the formula for the simplified conical seamount case with constant slope just described. They argue from the $1/\alpha^2$ dependence that because the slope is small near the top and bottom, the downward diapycnal flow of fluid near the top and bottom would be larger than midway along the seamount. For isopycnal surfaces around the base of the seamount,

this argument relies on the buoyancy flux remaining large at large distance from the seamount so that the area of the annulus of significant mixing on an isopycnal surface increases with increasing depth, leading to net downward flow, through (4).

However, a real seamount typically sits on an abyssal plain. At large enough distance two effects are likely to disturb the scenario above. One is that buoyancy flux at the top of the boundary layer above an abyssal plain is likely to be much weaker than near the seamount where topographic effects enhance turbulence generation. The other is that at some distance from the seamount the slope must go through zero, and some aspect of the analysis must break down. Possibilities are that the density field is not cylindrically symmetric or that neutral density surfaces cannot be regarded as flat so that extrapolating the buoyancy flux into the interior using the local bottom slope is not accurate. As an alternative, I offer the following analysis of mixing on the flanks of a seamount bounded by a cylindrical control volume. An important difference from the scenarios of MF17 is that buoyancy fluxes are specified to vanish at the edge of the control volume and beyond.

For such a seamount confined within a cylindrical control volume, the area of integration of the buoyancy flux would be that of an annulus between an inner radius r_i at the intersection of the isopycnal surface and the top of the boundary layer and the lesser of the radius R of the control volume and an outer radius r_o at which the buoyancy flux becomes negligible because the height above the bottom of the isopycnal surface becomes large. When $r_o < R$ the area of this annulus is $\pi(r_o^2 - r_i^2)$ and the situation is as envisioned by MF17. But when $r_o > R$, r_o is replaced by R in this formula. As noted above, MF17 argue that dF_B/db is likely to be less than zero because of the shrinking area of the annulus of significant mixing with height, so that $\varepsilon_{\mathrm{NET}}$ is negative (i.e., flow is downward). This is likely to be true at midlevels along a seamount where $r_o < R$. However, in the neighborhood of the buoyancy surface that enters the region at the top of the boundary layer at $r = R$, dF_B/db is positive, dominated by the rapidly increasing area of buoyancy surfaces with height. The absolute value of any contribution to dF_B/db from the boundary layer is smaller by a factor on the order of λ_{BL}/R, where λ_{BL} is the length of the curve of intersection of the isopycnal surface with the r–z plane in the boundary layer. At greater heights, as r_o becomes less than R, the area of the annulus decreases with height, as in MF17, and F_B is likely to decrease with height; where this happens depends not only on the area of the annulus but also on the details of the turbulent buoyancy flux within that annulus. Thus, we anticipate a deep region where the overall effect of mixing is to lighten the water. Above that, the overall effect is to transfer buoyancy to deeper water.

To illustrate, consider the simplified case of flat isopycnals everywhere except in a bottom boundary layer of uniform depth in which the isopycnals are perpendicular to the bottom (Fig. 1a). The equations for conservation of mass and of density anomaly for such a situation (see appendix) require the flow in the r–z plane to be that shown in Fig. 1a. The small contribution to dF_B/db within the boundary layer has been neglected in this calculation.

No attempt is made here to satisfy the momentum equations. There is a venerable series of studies of flow associated with mixing in the neighborhood of sloping boundaries on a rotating planet, reviewed, for example, by Garrett et al. (1993). Analytical solutions have been obtained for simple situations, such as constant stratification in the far field, uniform slope, and independence of the field in the along-slope direction. Distortion of isopycnal surfaces associated with cross-slope and along-slope flows arise, which depend on the choice of eddy diffusivities and viscosities. However, the simple geometry chosen here is taken as a crude approximation to more realistic geometries. Diffusive and advective fluxes across these surfaces must conserve mass and buoyancy. These fluxes depend on the rather arbitrary choice of how the diffusivity varies as a function of buoyancy. We shall see that the main features of the cross-slope flow in the dynamical models are present in this simplified model, as they depend primarily on the continuity and buoyancy equations.

The vertical profile of turbulent buoyancy flux used here is a decaying exponential function of height above the top of the boundary layer, with scale height 500 m, as for some of the cases treated by MF17. However, in the present case we specify that the buoyancy flux at the top of the boundary layer be proportional to $\cos(\pi r/2R)$ within the domain and zero beyond the domain, to be clear about the effect of negligible buoyancy flux far from the seamount. The vertical density profile used (Fig. 1b, dashed line) is typical of the deep ocean. A bottom boundary layer with zero potential density gradient normal to the bottom and of uniform thickness of 49 m is imposed. The thickness of the boundary layer chosen and even along-slope variations in thickness have no influence on the volume flux in the boundary layer or on the interior flow in this model (see appendix); a constant boundary layer thickness has been chosen for convenience. The upslope flow entering the bottom boundary layer at radius R is zero because the buoyancy flux at the top of the boundary layer is zero there; geothermal flux being ignored. The bottom flow

increases toward the seamount at first owing to the increasing buoyancy flux at the top of the boundary layer, reaching a maximum of $0.4\,\mathrm{cm\,s^{-1}}$ at a radius of a little less than 18 km, but within that radius the bottom flow decreases as the seamount is approached because of increasing slope and increasing vertical buoyancy gradient.

The divergence of bottom flow between R and the radius of maximum bottom flow is balanced by a thin layer of inflow just above the boundary layer, exemplified by the large horizontal velocity vector at $r = 20$ km, $z = 5450$ m in Fig. 1a. Convergence of fluid in the bottom boundary layer within the radius of maximum bottom flow is balanced by an outward flow in the layers above the boundary layer. The flow in the interior, shown in Fig. 1a as lighter vectors, has a downward, diapycnal component everywhere except at the outer edge, as expected. The magnitude of the flow diminishes strongly with height. Above 4700 m, the flow is very weak, still with a downward component and generally toward the seamount. As Figs. 1a,b (solid line) show, fluid is imported into the domain just above the boundary layer, exported in a layer above that, and weakly imported again further aloft. Thus, the density of bottom water is decreased at the expense of buoyancy of the fluid in the interior.

The mass leaving the control volume is within 1% of the mass entering in the numerical calculation. The velocity-weighted neutral density leaving the control volume through the sides is within $10^{-4}\,\mathrm{kg\,m^{-3}}$ of the velocity-weighted neutral density entering through the sides and top of the control volume. As already noted, these two velocity-weighted neutral densities should be the same because, other than a very weak turbulent flux at the top of the domain and geothermal heat that is ignored here, turbulent mixing around the seamount can only redistribute density within the domain. The small departures from mass and density conservation are due to approximations inherent in the numerical calculation.

Figure 1c shows the vertical profile of F_B, the total downward turbulent buoyancy flux across isopycnal surfaces outside the boundary layer, and the total flow through isopycnal surfaces $\varepsilon_{\mathrm{NET}}$ from (4). The graph of $\varepsilon_{\mathrm{NET}}$ is dominated by the spike of upward flow in the layer just above the boundary layer. The layer in which the flow is to lighter density is about 290 m thick. The $\varepsilon_{\mathrm{NET}}$ continues to decrease above this layer, becoming more negative until it reaches a minimum at around 4900-m depth. In this layer of convergence of $\varepsilon_{\mathrm{NET}}$ mass conservation requires the radial component of the velocity at $r = R$ to be outward. Let us call this the "export layer." Above this export layer $\varepsilon_{\mathrm{NET}}$ is still downward, as argued by MF17, but its magnitude decreases with height so that the flow at $r = R$ is inward. Thus, bottom water, flowing toward the seamount, is lightened at the expense of buoyancy from the layer just above it, in which flow is away from the seamount. The velocity-weighted density of the water in the export layer in this simple model is $0.002\,\mathrm{kg\,m^{-3}}$ less than the density of the water entering in the thin layer above the bottom boundary layer. This imbalance of density flux is compensated by the very weak inward flow of light water above the export layer.

Some of the key features of the cross-slope flow derived in the dynamical analytical models of the circulation in the neighborhood of a sloping bottom mentioned earlier (Garrett et al. 1993) are evident here. There is a cross-slope secondary circulation, with diapycnal flow generally toward the seamount and to lighter isopycnals in a bottom layer and flow generally away from the seamount and to denser isopycnals above this layer. The integrals of the fluxes of mass and buoyancy integrated along any cylindrically symmetric surface from the bottom to the top of the control volume are zero. Diapycnal diffusive fluxes within the boundary layer are not specified beyond that this flux go from its value just above the top of the boundary layer to zero at the bottom of the boundary layer, and so the question of whether stratification and diffusivity within the boundary are important is moot. Important features that are included here but generally not in the analytical models are that the slope and the buoyancy flux at the top of the boundary layer vary with cross-slope distance. Also, the buoyancy gradient in the far field is not independent of z. Because of radial variations of the slope and diffusivity at the top of the boundary layer, fluid is variously drawn into the boundary layer and expelled from it, and modification of water masses by mixing within the control volume is thereby communicated to the interior.

Omitted from the present analysis, however, is distortion of isopycnal surfaces associated with dynamical balances between Coriolis, pressure gradient, and viscous forces. As already noted, the present analysis for volume fluxes is insensitive to along-slope variations in the boundary layer thickness. Convergences of turbulent buoyancy flux in the boundary layer not balanced by the mean along-slope diapycnal flow are neglected here, as well as in MF17, and in the analytical models, the latter of which generally have uniform fluxes in the along-slope direction. The present results would be sensitive to vertical distortions of isopycnal layers in the interior in that if dissipation (and therefore diapycnal velocity) is prescribed as a function of z then such distortions will influence the mass budgets of isopycnal layers through the divergence of the diapycnal velocity. In particular (A15) in the appendix would have to be

changed to an equation for mass conservation in an isopycnal layer rather than a horizontal layer. This would change the details of the interior circulation. However, given the uncertainty in the actual spatial distribution of the dissipation, this does not seem to be a serious shortcoming for the present purpose. A sensible refinement that is beyond the present scope might be to use actual observed isopycnal surfaces and best estimates from internal wave dynamics and measurements of turbulent dissipation to infer the cross-slope circulation. Then one might try to insist that the eddy viscosity and along-slope velocities be such that the momentum equations are satisfied.

The volume flux entering just above the boundary layer in this simple illustration is 0.022 Sv (1 Sv $\equiv 10^6\,\mathrm{m^3\,s^{-1}}$). Hence the effect of mixing around the seamount is to reduce the density of this amount of water by about $0.002\,\mathrm{kg\,m^{-3}}$. One can imagine water exported from one seamount becoming bottom water for another, to be further lightened, and thus seamounts can collectively contribute positively to the overturning circulation of the deep water. For example, if this simple model had quantitative validity, 100 such seamounts could reduce the density of 2.2 Sv of bottom water by $0.002\,\mathrm{kg\,m^{-3}}$, which is a sizable fraction of the spread in density of northward-flowing bottom water in the lower cell of the global meridional overturning circulation presented by Lumpkin and Speer (2007, their Fig. 2). Thus, 100 seamounts could conceivably contribute significantly to conversion of deep northward-going water to less deep southward-going water in the deep cell.

The same pattern of bottom water modification as for the seamount case can occur along a linear midocean ridge, a consideration that motivated the present comment because of experience from the Brazil basin (see Polzin et al. 1997; Ledwell et al. 2000; St. Laurent et al. 2001). MF17 considered the case of a linear ridge (their section 6), showing that for a constant slope (all the way to infinite depth) and constant scale height for the buoyancy flux, there is no net flow ($\varepsilon_{\mathrm{NET}} = 0$) unless the buoyancy flux at the top of the boundary layer increases with increasing buoyancy (i.e., upward along the boundary layer). The following illustration shows that, like the seamount case, a more realistic ridge shape leads to lightening of bottom water. Again, it is assumed that diapycnal mixing and advection go to zero at the edge of the control volume, and this again is an important difference from MF17. This approximation is supported in the case of the Brazil basin, by the observation that turbulent dissipation rates are very small over the abyssal plain west of the region of abyssal ridges and canyons at that site (Polzin et al. 1997).

Figure 2a shows the circulation near a ridge in the cross-ridge plane that satisfies mass and buoyancy conservation, again with the simple cross-slope shape of isopycnal surfaces used for the seamount and no attempt made to satisfy momentum equations. The shape of the bottom is a smoothed version of the western flank of the Mid-Atlantic Ridge in the Brazil basin, where canyon walls and abyssal hills can serve as baffles and strong sources of friction. The bottom boundary layer thickness and profiles of buoyancy flux and density have all been taken to be the same as for the seamount case. Buoyancy flux at the top of the boundary layer is again taken to fall to zero at the edge of the control volume as $\cos(\pi x/2L)$ (where $x = -L = -1000\,\mathrm{km}$ delimits the control volume) and to be zero beyond $x = -L$. Such a ridge is much more effective at lightening bottom water than the seamount. The influx in a 440-m-thick layer above the boundary layer at the left edge of the control volume is $0.0019\,\mathrm{Sv\,km^{-1}}$. The fluid leaving the region in the 520-m-thick layer above is lighter by about $0.028\,\mathrm{kg\,m^{-3}}$. In this scenario, a 1000-km stretch of ridge could lighten 1.9 Sv of bottom water by $0.028\,\mathrm{kg\,m^{-3}}$. This would be a major contribution to the deep overturning cell estimated in Lumpkin and Speer (2007). Of course, the above calculations are only illustrations, as the density field and buoyancy flux field have been oversimplified.

The ridge in Fig. 2 could be viewed as a linear stretch of continental slope up to about 3000-m depth. Most of the water-mass modification takes place below this level. Hence, a stretch of continental slope might have an effect on the bottom water similar to that of a midocean ridge. Bottom water would be imported and slightly lighter ''deep water'' would be exported. To balance the buoyancy budget, a relatively small amount of water above the export layer would be imported. It seems that regardless of whether a seamount, a ridge, or a continental slope is considered, the effect of mixing is confined mostly to the bottom water, which becomes lighter, and the deep water overlying the bottom water, which becomes denser. Thus, with downward-increasing buoyancy flux, mixing near the bottom contributes positively to the lightening of bottom water and densification of water just above (i.e., to homogenization of the bottom and deep water), as recognized in a more global context in the work of de Lavergne et al. (2016). Perhaps density in the deep cell is lightened by water moving from one locale to another along a ridge or continental slope, deep water from one site becoming bottom water at the next site, to be further lightened, as envisioned above for the seamount case. It is worth noting as an aside that steady-state flow along a flat or gently sloping bottom can be a continuous, simple example of this progressive lightening of bottom water if

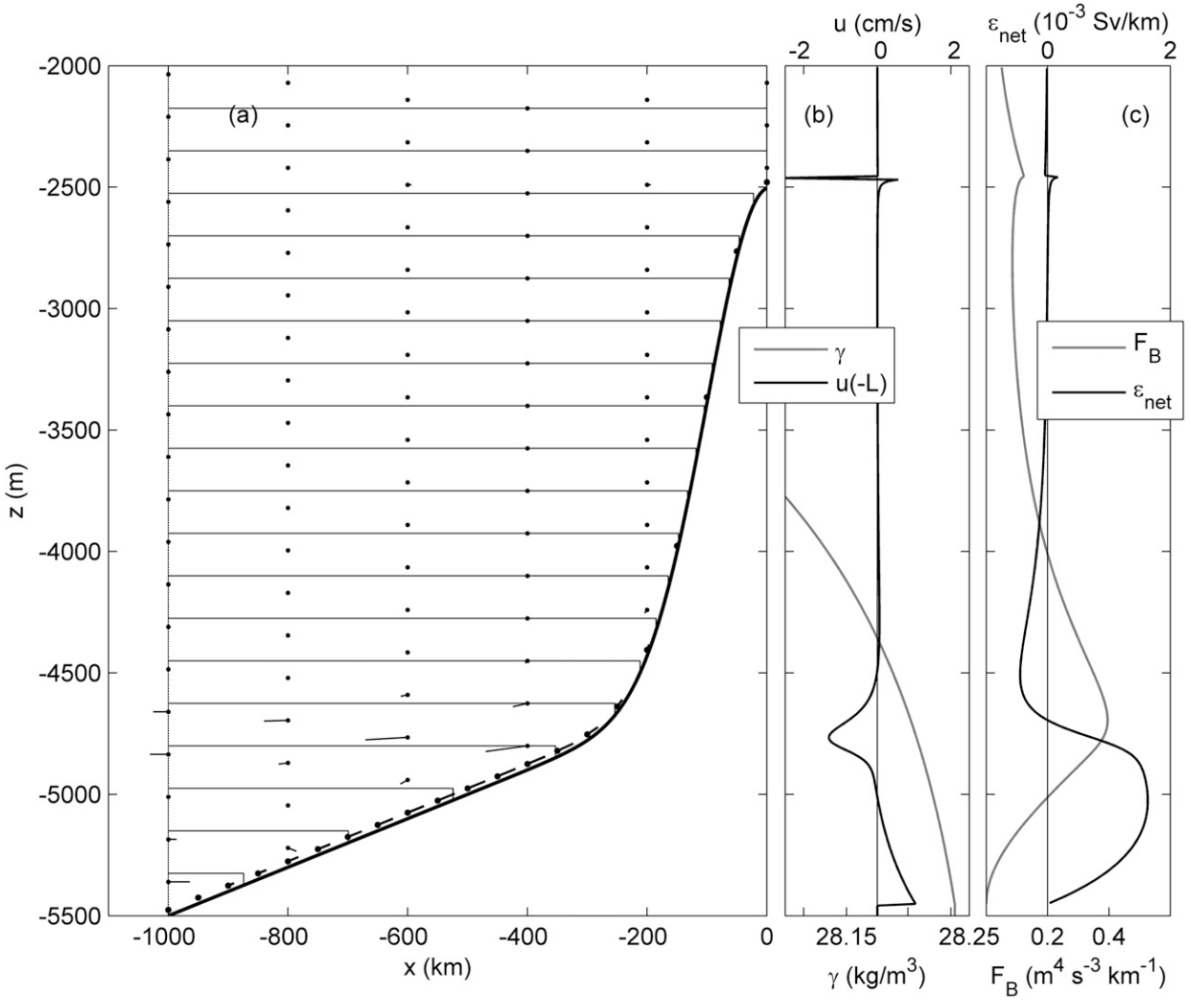

FIG. 2. Idealized flow on the flanks of a linear ridge. (a) The heavy black line shows the bottom, while the light lines show isopycnal surfaces. The vertical line at $x = -1000$ km shows the left edge of the model domain. Line segments represent velocity vectors, with a dot at their tails. The length of the vectors in the bottom boundary layer have been reduced by a factor of 10 compared with those showing the flow in the interior. For scale, the velocity represented by the arrow at the left edge at $z = -5330$ m is 0.63 cm s^{-1} and the maximum bottom velocity, near $x = -440$ km, is 6 cm s^{-1}. The depth of the bottom boundary layer is uniform at 49 m. (b) The horizontal velocity u at the outer boundary of the domain is shown as a black line (top axis; the vertical line is at $u = 0$ for reference). The neutral density used in the calculation is shown below 3800 m as a gray line (bottom axis). Diapycnal diffusivity, and therefore the boundary layer velocity, is 0 at $x = -1000$ km, by construction. Between 5450- and 5000-m depth bottom water is imported into the domain. Above this layer, up to 4500 m, fluid is exported. Above 4500 m fluid is weakly imported. Flows near the level of the peak are enhanced because of the small slope, large dissipation rate, and condition that $u = 0$ at the top. (c) The gray line shows the integral in the $x-z$ plane of the diffusive flux F_B (bottom scale), and the black line shows the integrated upward diapycnal volume flux $\varepsilon_{\mathrm{NET}}$ (top scale), with a fine line at $\varepsilon_{\mathrm{NET}} = 0$ shown for reference.

the flow is perpendicular to isopycnal surfaces that approach the bottom at a glancing angle. These effects can in fact be seen in the global analysis of de Lavergne et al. (2016, e.g., in their Fig. 6a), where deep neutral density surfaces slope downward to the north and zonally integrated buoyancy fluxes through those surfaces, estimated from a simple formula for the dissipation of turbulence generated by internal tides, increasingly shift from upward to downward from south to north.

These considerations lead one to conclude that mixing around seamounts and ridges can contribute positively to the deep cell of the overturning circulation. They also suggest that it may be misleading to focus too much on the behavior of the perimeter of the ocean basins with depth in understanding the deep overturning

circulation. As MF17 recognize, what is important is the perimeter of isopycnal surfaces, for which the perimeter of level surfaces is sometimes a poor approximation. Although the isopycnal surfaces drawn in the examples here are flat, it is easy to imagine similar cases for which the bottom is flat and the isopycnal surfaces are sloped to meet it. The important angle is that of mean isopycnal surfaces relative to the bottom, in combination with the spatial distribution of turbulent buoyancy fluxes.

MF17 show convincingly that the net global flow across isopycnal surfaces is a rather small difference between large diapycnal flow to high density in the interior and larger diapycnal flow to low density in the boundary layer. The average diapycnal diffusivity required at the top of the boundary layer to close the deep cell of the overturning circulation was estimated by them to have the rather large value of $5 \times 10^{-3}\,\mathrm{m^2\,s^{-1}}$, based on the gross perimeter of the continents, estimated at $5 \times 10^{7}\,\mathrm{m}$. It seems, however, that the perimeter of midocean ridges was not included in this estimate, and mixing around seamounts were argued to increase the demand for mixing along the continental slopes rather than reduce it. If midocean ridges are included, a revised estimate of the perimeter of isopycnal surfaces below 2500-m depth is perhaps $2 \times 10^{8}\,\mathrm{m}$, 4 times greater than used by MF17. This reduces the required diffusivity at the top of the boundary layer proportionally. Seamounts might reduce the required diffusivity further, as noted above. Also, as noted above, isopycnal surfaces can approach the bottom over abyssal plains at a glancing angle, leading to a strong increase in area of isopycnal surfaces with increasing buoyancy, though, admittedly, turbulent buoyancy fluxes over abyssal plains are probably small. [More importantly for abyssal plains, de Lavergne et al. (2016) found that geothermal heating provides a large fraction of the buoyancy gain required for "consumption" of Antarctic Bottom Water.] Thus, recognition of turbulent fluxes around seamounts and especially midocean ridges, and perhaps even along abyssal plains, can reduce the average diapycnal diffusivity at the top of the boundary layer over the continental slopes required to close the deep cell of the meridional overturning circulation. In particular, mixing on the flanks of the global midocean ridge system seems especially likely to play a crucial positive role, given, for example, the observational evidence for enhanced mixing over the broad eastern flank of the Mid-Atlantic Ridge in the Brazil basin.

Acknowledgments. Discussions with T. McDougall and R. Ferrari have been very helpful. This work was supported by National Science Foundation Grant OCE-1232962.

APPENDIX

Idealized Model for the Flow Toward a Seamount and Ridge

The bottom around the seamount of Fig. 1 was given an analytical form for convenience:

$$z_b = ar + H_s \exp\left[-r^2/(2L_s^2)\right], \tag{A1}$$

where the radial coordinate r ranges from 0 to $R = 20\,\mathrm{km}$, which is the outer radius of a control volume enclosing the seamount. The above equation describes a Gaussian peak added to a uniformly sloping bottom. The parameters chosen for the seamount example (underlying slope $a = -2 \times 10^{-3}$; peak height $H_s = 3000\,\mathrm{m}$; and rms peak width $L_s = 5000\,\mathrm{m}$) were based on the shape of an unnamed seamount southwest of the Hawaiian Ridge at approximately 179.8°W, 26.3°N, which seemed typical for midocean seamounts.

The dissipation of turbulent kinetic energy ε is a function of height above bottom and distance from the peak of the seamount, with the following form:

$$\varepsilon = \varepsilon_b \exp\left[-(z - z_b)/H_\varepsilon\right] \cos\left(\frac{\pi}{2}\frac{r}{R}\right). \tag{A2}$$

We use $\varepsilon_b = 10^{-8}\,\mathrm{W\,kg^{-1}}$ and $H_\varepsilon = 500\,\mathrm{m}$, guided by the results from the Brazil basin (St. Laurent et al. 2001). Thus, ε falls off exponentially with height above bottom, but here ε also falls to zero at the boundary of the control volume, as a cosine function. The downward flux of buoyancy above the bottom boundary layer is assumed to be given by the formula of Osborn (1980), with a constant value for the mixing efficiency $\Gamma = 0.2$:

$$kN^2 = \Gamma\varepsilon, \tag{A3}$$

where N^2 is the square of the buoyancy frequency, given by

$$N^2 = -\frac{g}{\rho}\frac{d\gamma}{dz} = \frac{db}{dz}, \tag{A4}$$

where g is the acceleration due to gravity, ρ is a reference seawater density, γ is the neutral density, and b is the buoyancy.

Thus, the diapycnal diffusivity k for buoyancy or density is given by

$$k = -\frac{\rho}{g}\left(\frac{d\gamma}{dz}\right)^{-1}\Gamma\varepsilon. \tag{A5}$$

Neutral density above the boundary layer is taken to be a function only of z:

$$\gamma = \gamma_b - \Delta\gamma \exp(z/H). \tag{A6}$$

Values of $\gamma_b = 28.27\,\mathrm{kg\,m^{-3}}$, $\Delta\gamma = 7.4\,\mathrm{kg\,m^{-3}}$, and $H = 1000\,\mathrm{m}$ give a realistic density profile in the bottom and deep water of interest here. The density in a bottom boundary layer of uniform thickness $h_b = 49\,\mathrm{m}$ is approximated as constant along the normal to the bottom and equal to the density given by (A6) at the top of the boundary layer. Lines of constant neutral density are thus level above the top of the boundary layer. At the top of the boundary layer, isopycnal lines bend down abruptly to intersect the bottom at right angles (Fig. 1; the angle of intersection with the bottom is distorted by the vertical exaggeration of the figure).

A steady-state flow confined to the two dimensions of the r–z plane of Fig. 1 is determined from the continuity equation, the density equation, and (A5) for diapycnal diffusivity, for the specified density field and spatial distribution of ε. The momentum equations are not invoked but can be imagined to be satisfied by unspecified friction and slight pressure gradients associated with small slopes of isopycnals above the boundary layer.

The diapycnal velocity above the top of the boundary layer satisfies the steady-state density equation:

$$w = \left(\frac{d\gamma}{dz}\right)^{-1}\frac{\partial}{\partial z}\left(k\frac{d\gamma}{dz}\right) = -\frac{\rho}{g}\left(\frac{d\gamma}{dz}\right)^{-1}\Gamma\frac{\partial\varepsilon}{\partial z}, \tag{A7}$$

where (A5) has been used in the second equality. It is this last equation from which it is argued that if ε decreases upward then the diapycnal velocity must be downward.

The density within the boundary layer is approximated as being equal to the density γ_t at the top of the boundary layer. The steady-state density equation integrated from the bottom to the top of the bottom boundary layer along an isopycnal is then

$$\frac{d}{dr}(ru_bh_b\gamma_t) = -rw_t\gamma_t + rk_t\left(\frac{d\gamma}{dz}\right)_t, \tag{A8}$$

where u_b is the along-slope velocity in the boundary layer, averaged over the isopycnal for which $\gamma = \gamma_t$; w_t is the vertical velocity at the top of the boundary layer, approached from below; k_t is the diapycnal diffusivity from (A5) at the top of the boundary layer; and $(d\gamma/dz)_t$ is the density gradient at the top of the boundary layer, approached from above. Geothermal flux has been ignored. Note that in (A8) and (A9) the attenuation of vertical fluxes by the sine of the angle between the vertical axis and the sloping top of the boundary layer is exactly compensated by the increased length of an area element between r and $r + dr$ owing to the slope.

The product of γ_t and the mass conservation equation for the boundary layer, given by

$$\gamma_t\frac{d}{dr}(ru_bh_b) = -r\gamma_tw_t, \tag{A9}$$

is subtracted from (A8) to obtain

$$u_bh_b\frac{d\gamma_t}{dr} = k_t\left(\frac{d\gamma}{dz}\right)_t. \tag{A10}$$

The geometry of the lines of constant density is such that

$$\frac{d\gamma_t}{dr} = \alpha\left(\frac{d\gamma}{dz}\right)_t, \tag{A11}$$

where α is the bottom slope, obtained by differentiating (A1) with respect to r.

Thus we arrive at this simple result:

$$u_bh_b = \frac{k_t}{\alpha}. \tag{A12}$$

That is, the volume flux in the bottom boundary layer is simply proportional to the diffusivity at the top of the boundary layer and inversely proportional to the bottom slope. If the bottom were flat (i.e., $\alpha = 0$) anywhere in the system, then some feature of this illustration must be abandoned. For example, steady-state, cylindrical symmetry, or flat isopycnal surfaces, could be given up. Note that u_b and h_b appear in the above development only as their product, the volume flux. The development and the interior circulation does not depend on u_b and h_b separately. In fact, the thickness of the boundary layer could vary along the bottom in the radial direction; the only modification needed would be that α should be the slope of the top of the boundary layer rather than of the bottom [see (A11)].

From (A9) and (A12) we have the following:

$$w_t = -\frac{1}{r}\frac{d}{dr}\left(\frac{rk_t}{\alpha}\right) = -\frac{d}{dr}\left(\frac{k_t}{\alpha}\right) - \frac{1}{r}\frac{k_t}{\alpha}. \tag{A13}$$

In the present case the volume flux $2\pi ru_bh_b$ in the boundary layer is toward the seamount everywhere and increases from zero at $r = 20\,\mathrm{km}$ to a maximum at r a little less than 18 km, so that w_t is negative in that range (i.e., fluid must be supplied to the boundary layer from above). At smaller radii the volume flux decreases as r decreases so that w_t is positive there; the boundary layer is a source of fluid to the interior. The vertical velocity just above the top of the boundary layer, which will be called w_+, is given by (A7) and is always downward. The discontinuity in vertical velocity at the top of the boundary layer between w_t and w_+ that results must be balanced by a horizontal (i.e., epipycnal) flow entering or emanating from the sloping top of the boundary layer, given by the following (see Fig. A1; note that $\alpha < 0$ as it is defined):

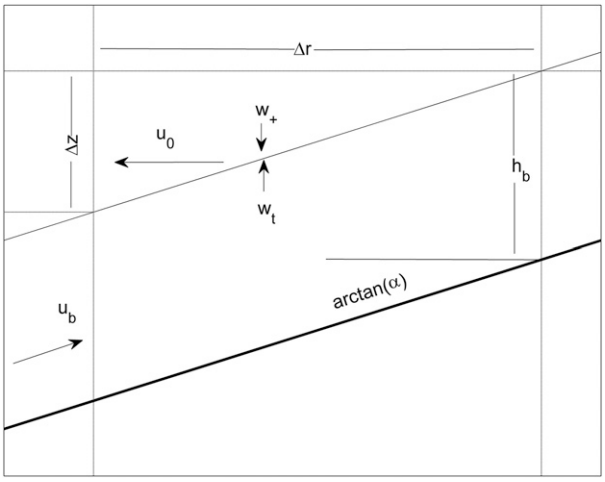

FIG. A1. Geometry justifying (A14). The heavy line is the bottom, with slope $dz_b/dr = \alpha$. The top of the boundary layer is parallel to the bottom at height h_b. Volume flow per radian in the boundary layer is ru_bh_b. Convergence of this flow must be balanced by the vertical flow $rw_t\Delta r$. But just above the top of the boundary layer there is downward flow $rw_+\Delta r$. This convergence at the lid of the boundary layer must be balanced by $ru_0\Delta z$. So $u_0\Delta z = (w_t - w_+)\Delta r$, which gives (A14) since $\Delta z/\Delta r = -\alpha$.

$$u_0 = -(w_t - w_+)/\alpha. \tag{A14}$$

The horizontal velocity at radius r at a given depth is then given by integrating the divergence of the vertical velocity, as calculated from (A7), which in cylindrical coordinates gives

$$u(r,z) = u_0 - \frac{1}{r}\int_{r_0}^{r} \frac{\partial w}{\partial z} r' dr', \tag{A15}$$

where r_0 is the value of r where the top of the boundary layer is at z. Symmetry requires $u = 0$ at $r = 0$ above the boundary layer at the top of the seamount, so (A15) is used at those levels with $u_0 = 0$ and $r_0 = 0$. The velocity field has been calculated numerically, with a simple finite-difference scheme, from the above equations and parameter choices with a grid of 400 vertical layers by 2400 radial intervals, giving the flow pattern shown in Fig. 1.

The equations for the flow in the ridge case are the same as those above, except that cylindrical coordinates are no longer needed so that r may be set to a constant and eliminated in (A8) and (A9); then r may be replaced by x, the cross-ridge distance, throughout, and the analog of (A15) is

$$u(x,z) = u_0 - \int_{x_0}^{x} \frac{\partial w}{\partial z} dx'. \tag{A16}$$

Figure 2 shows the results of the numerical calculation, again with 400 vertical layers and 2400 horizontal intervals. The setup for the ridge case was the same as for the seamount case, except that the distance from the outer edge of the control volume to the ridge crest is 1000 km, and in (A1) for the bottom shape the values used were $a = 10^{-3}$, $H_s = 2000$ m, and $L_s = 100$ km, roughly appropriate for the eastern flank of the Mid-Atlantic Ridge in the Brazil basin.

REFERENCES

de Lavergne, C., G. Madec, J. L. Sommer, A. J. G. Nurser, and A. C. Naveria Garabato, 2016: On the consumption of Antarctic Bottom Water in the abyssal ocean. *J. Phys. Oceanogr.*, **46**, 635–661, https://doi.org/10.1175/JPO-D-14-0201.1.

Ferrari, R., A. Mashayek, T. J. McDougall, M. Nikurashin, and J.-M. Campin, 2016: Turning ocean mixing upside down. *J. Phys. Oceanogr.*, **46**, 2239–2261, https://doi.org/10.1175/JPO-D-15-0244.1.

Garrett, C., P. MacCready, and P. Rhines, 1993: Boundary mixing and arrested Ekman layers: Rotating stratified flow near a sloping boundary. *Annu. Rev. Fluid Mech.*, **25**, 291–323, https://doi.org/10.1146/annurev.fl.25.010193.001451.

Klocker, A., and T. J. McDougall, 2010: Influence of the nonlinear equation of state on global estimates of dianeutral advection and diffusion. *J. Phys. Oceanogr.*, **40**, 1690–1709, https://doi.org/10.1175/2010JPO4303.1.

Ledwell, J. R., E. T. Montgomery, K. L. Polzin, L. C. St. Laurent, R. W. Schmitt, and J. M. Toole, 2000: Evidence for enhanced mixing over rough topography in the abyssal ocean. *Nature*, **403**, 179–182, https://doi.org/10.1038/35003164.

Lumpkin, R., and K. Speer, 2007: Global ocean meridional overturning. *J. Phys. Oceanogr.*, **37**, 2550–2562, https://doi.org/10.1175/JPO3130.1.

McDougall, T. J., 1989: Dianeutral advection. *Parameterization of Small-Scale Processes: Proc. Fifth 'Aha Huliko'a Hawaiian Winter Workshop*, Honolulu, HI, University of Hawai'i at Mānoa, 289–316.

——, and R. Ferrari, 2017: Abyssal upwelling and downwelling driven by near-boundary mixing. *J. Phys. Oceanogr.*, **47**, 261–283, https://doi.org/10.1175/JPO-D-16-0082.1.

Osborn, T. R., 1980: Estimates of the local rate of vertical diffusion from dissipation measurements. *J. Phys. Oceanogr.*, **10**, 83–89, https://doi.org/10.1175/1520-0485(1980)010<0083:EOTLRO>2.0.CO;2.

Polzin, K. L., J. M. Toole, J. R. Ledwell, and R. W. Schmitt, 1997: Spatial variability of turbulent mixing in the abyssal ocean. *Science*, **276**, 93–96, https://doi.org/10.1126/science.276.5309.93.

St. Laurent, L. C., J. M. Toole, and R. W. Schmitt, 2001: Buoyancy forcing by turbulence above rough topography in the abyssal Brazil basin. *J. Phys. Oceanogr.*, **31**, 3476–3495, https://doi.org/10.1175/1520-0485(2001)031<3476:BFBTAR>2.0.CO;2.